RSC Advances

PAPER

View Article Online
View Journal | View Issue

Cite this: *RSC Adv.*, 2017, **7**, 17748

Preparation of [^{18}F]-NHC-BF_3 conjugates and their applications in PET imaging†

Kantapat Chansaenpak,‡[ac] Mengzhe Wang,‡[a] Hui Wang,[a] Benjamin C. Giglio,[a] François P. Gabbaï,[b] Zhanhong Wu[a] and Zibo Li*[a]

Received 29th December 2016
Accepted 14th March 2017

DOI: 10.1039/c6ra28806e

rsc.li/rsc-advances

N-Heterocyclic carbene boron trifluoride (NHC-BF_3) conjugates were successfully radiofluorinated by $SnCl_4$-promoted ^{18}F–^{19}F isotopic exchange reaction in one labelling step. This method afforded *in vivo* stable PET agents that efficiently bound to targeted tumours yielding PET images with good tumour-to-background contrast.

Fluorine-18 is typically incorporated into molecular tracers at the last step of the overall synthesis process due to its short half-life (110 minutes). One of the recent methods for late-stage radiofluorination is a pre-functionalization approach in which a ^{18}F-captor such as a BF_3 or a BF_2 unit is preinstalled into bioactive molecules.[1] Several examples, including the radiofluorinations of alkylammoniomethyltrifluoroborate[2] ($AMBF_3$) (Scheme 1A), BODIPY[3] (Scheme 1B) and phosphonium aryltrifluoroborate[4] ($PArBF_3$) (Scheme 1C) conjugates, were demonstrated.

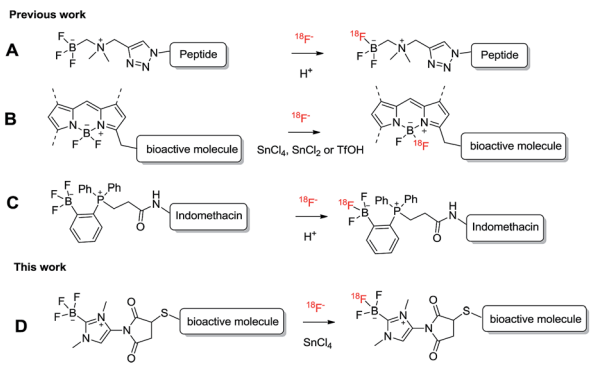

Scheme 1 Scheme showing the late-stage radiofluorinations of boron-based radiotracers shown in previous reports (A–C) and this report (D).

In the case of $AmBF_3$ and $PArBF_3$ conjugates, the ^{18}F–^{19}F isotopic exchange of the BF_3 moiety could be simply processed in acidic aqueous media.[2d,4,5] However, the ^{18}F–^{19}F isotopic exchange of the BF_2 unit in BODIPY conjugates could only be efficiently done in a dried organic solvent with strong Lewis/BrØnsted acid promotors ($SnCl_4$, $SnCl_2$, or TfOH).[3,6]

Recently, we demonstrated that the [^{18}F]-maleimide functionalized NHC-BF_3 ([^{18}F]**1**) (Fig. 1) could be prepared *via* $SnCl_4$-promoted ^{18}F–^{19}F isotopic exchange and it could be easily conjugated to Cys-Phe dipeptide.[7] However, the ^{18}F direct labelling of the NHC-BF_3 pre-functionalized bioactive molecule (Scheme 1D) has not been reported. With this in mind, we decided to validate the late-stage radiofluorination in NHC-BF_3 conjugated bioactive molecules, including glutamate–urea–lysine (**2**), cyclic RGD-containing peptide (**3**), and neurotensin (NT) peptide (**4**) (Fig. 1). The results on radiosynthesis and PET imaging of these [^{18}F]-NHC-BF_3 conjugates are presented in this report.

As a starting point, NHC-BF_3 conjugated glutamate–urea–lysine (**5**), cyclic RGD-containing peptide (**6**), and neurotensin

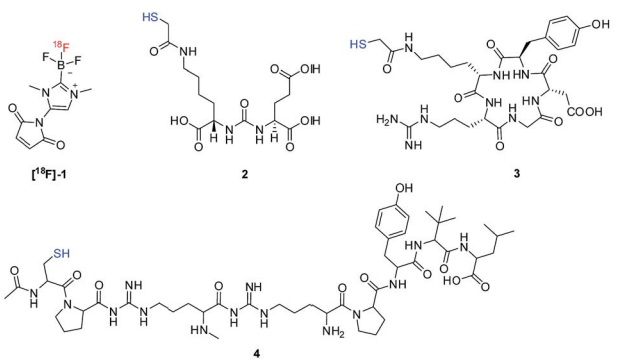

Fig. 1 Chemical structures of maleimide functionalized NHC-BF_3 adduct (**1**) and thiol containing bioactive molecules (glutamate–urea–lysine (**2**), cyclic RGD-containing peptide (**3**) and neurotensin peptide (**4**)) studied in this work.

[a]*Biomedical Research Imaging Center, Department of Radiology, University of North Carolina, Chapel Hill, North Carolina, USA 27514. E-mail: ziboli@med.unc.edu*
[b]*Department of Chemistry, Texas A&M University, College Station, Texas, USA 77843*
[c]*National Nanotechnology Center (NANOTEC), National Science and Technology Development Agency (NSTDA), 111 Thailand Science Park, Pathum Thani, Thailand 12120*

† Electronic supplementary information (ESI) available. See DOI: 10.1039/c6ra28806e

‡ These two authors contributed equally to this work.

peptide (7) were prepared by thiol-Michael addition click reaction of **1** with **2**, **3**, and **4**, respectively (Scheme 2). This reaction was performed by mixing the solution of **1** in MeCN with the solution of **2**, **3**, or **4** in phosphate buffer solution (PBS) pH 7.5. The reaction mixture was then incubated at room temperature for 2 hours before purifying with high-performance liquid chromatography (HPLC). The detection of the molecular ions by positive-mode electrospray mass spectrometry at *m*/*z* 653.1999 for **5**, 953.3689 for **6** and 1332.6725 for **7** confirmed the identity of the conjugates.

Next, we labelled our new NHC-BF_3 conjugates by $SnCl_4$-promoted ^{18}F–^{19}F isotopic exchange reaction. The solution of NHC-BF_3 conjugates and tin(IV)chloride (excess) in anhydrous MeCN was mixed with azeotropically dried tetrabutylammonium [^{18}F]-fluoride (TBAF) (Scheme 2). The mixture was heated at 70 °C for 10 min, then quenched with 1 mL of water and passed through a Sep-Pak light alumina N cartridge to remove an unreacted ^{18}F-fluoride.

The radio-HPLC profiles of [^{18}F]**5**, [^{18}F]**6** and [^{18}F]**7** obtained after passing through Sep-Pak alumina N cartridge are shown in Fig. 2A, C and D, respectively. The identity of [^{18}F]-NHC-BF_3 conjugates was confirmed by the comparison of their retention times with those of reference compounds as shown in Fig. 2A and B in the case of [^{18}F]**5**. The UV HPLC profiles of **6** and **7** are displayed in the ESI.† The radio-HPLC profiles revealed that the [^{18}F]**5**, [^{18}F]**6** and [^{18}F]**7** were obtained as a major product. The small radio-HPLC peaks of the impurities were also detected, which could be the results from decomposition due to exposure to $SnCl_4$. Although the HPLC purification is required, the radiolabelling time can be reasonably shortened compared with our previous report[7] as the radio-bioconjugation step between [^{18}F]-**1** and the bioactive molecule is removed.

The decay-corrected radiochemical yield, and specific activity for [^{18}F]**5**, [^{18}F]**6** and [^{18}F]**7** are shown in Table 1. The radiochemical yields ranging from 21.4 to 29.6% are comparable with those obtained from $SnCl_4$-promoted radiolabelling of BODIPY-RGD conjugate[3a] and slightly lower than $SnCl_2$ or TfOH-promoted radiolabelling of BODIPY conjugates reported in previous publications.[3] The specific activities of all [^{18}F]-

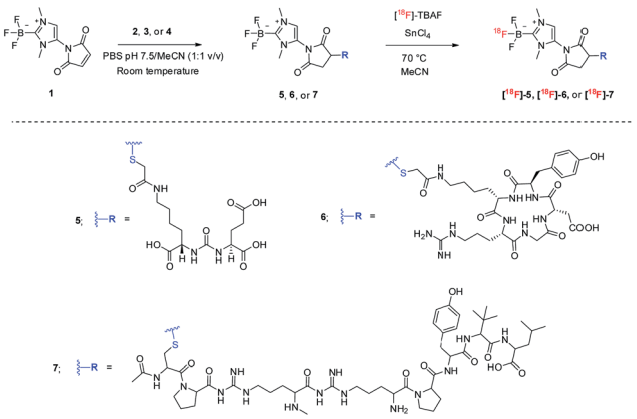

Scheme 2 Scheme showing the synthesis and the radiolabelling of **5**, **6**, and **7**.

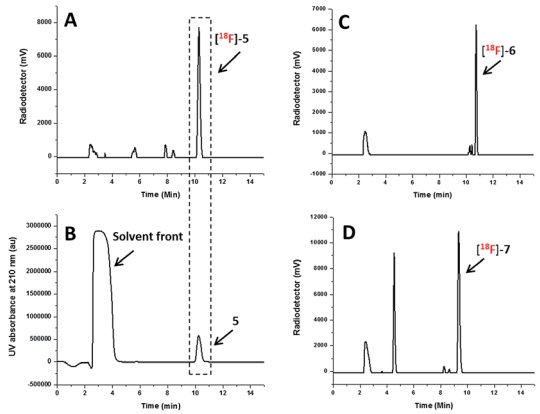

Fig. 2 Radio HPLC profile of the [^{18}F]**5** (A), [^{18}F]**6** (C) and [^{18}F]**7** (D) obtained after passing through Sep-Pak alumina N cartridge and UV HPLC profile of **5** (B) as the reference compound.

NHC-BF_3 conjugates are considerably higher than that of [^{18}F]-NHC-BF_3-Cys-Phe prepared by two-step radiosynthesis.[7]

In term of the *in vitro* stability, [^{18}F]**5**, [^{18}F]**6** and [^{18}F]**7** demonstrated negligible decomposition at both 60 and 120 min after incubation in phosphate buffer solution pH 7.5 under ambient temperature (Fig. 3 and ESI†). These results are consistent with the extremely long hydrolysis half-life of **1** observed by ^{19}F NMR spectroscopy and the *in vitro* stability studies of [^{18}F]-NHC-BF_3-Cys-Phe shown in the previous report.[7] Next, we chose [^{18}F]**5**, the prostate-specific membrane antigen (PSMA)-based radiotracer, to perform the *in vivo* stability study in mice.

The microPET/CT images obtained at 0.5 h and 4 h post injection revealed that [^{18}F]**5** mainly localized in kidneys due to its hydrophilic nature (Fig. 4), as seen with other PSMA-based radiotracers.[8] The high accumulation of [^{18}F]**5** in kidneys is partially due to high expression of PSMA within proximal renal tubules.[9] Based on PET quantification, the kidney uptake of [^{18}F]**5** was determined to be 12.1 and 2.3% ID per g at 0.5 h and 4 h post injection, respectively. This finding indicated that [^{18}F]**5** was slowly cleared from kidneys. Additionally, we did not observe any bone uptake signal due to tracer decomposition even at 4 h post injection which is similar to the *in vivo* stability of the [^{18}F]-NHC-BF_3-Cys-Phe.[7]

In order to validate whether these agents could be used for cancer imaging, the glioblastoma (U87MG) and pancreatic (PANC1) tumour bearing mice were injected with the radiolabelled RGD and NT conjugates, respectively. As shown in Fig. 5A–C, [^{18}F]**6** and [^{18}F]**7** nicely visualized tumour in a good contrast and showed negligible uptake in bone. Additionally, both tracers barely localized in liver due to the hydrophilic nature of the NHC-BF_3 conjugates which is different from the bio-distributions of the [^{18}F]-BODIPY-peptide conjugates[3a,6a] and the [^{18}F]-*ortho*-(Ph_2MeP)C_6H_4(BF_3)-indomethacin conjugate.[4] The target specificity of [^{18}F]**7** was confirmed by blocking experiment in which the radiotracer was co-injected with an excess amount (200 μg) of NT peptide (**4**). In this blocking experiment, the tumour uptake of [^{18}F]**7** was remarkably inhibited by nonradioactive NT peptide, confirming the

Table 1 Radiosynthetic results for [^{18}F]**5**, [^{18}F]**6** and [^{18}F]**7**

		Amount					
Entry	Cpd	μg	μmol	$SnCl_4$ (μL)	Temp. (°C)	RCY[a] (%)	SA[b] (GBq μmol^{-1})
1	[^{18}F]**5**	200	0.31	1	70	29.6	6.0
2	[^{18}F]**6**	300	0.32	1	70	25.6	3.5
3	[^{18}F]**7**	400	0.30	1	70	21.4	3.4

[a] Radiochemical yields (RCY) were calculated by dividing the ^{18}F-activity of the isolated product by the starting ^{18}F activity. [b] Specific activities (SA) were determined by dividing the isolated product activity by the amount of the product (based on the integration of UV-HPLC profile and compare it with the standard calibration curve). The radiochemical yields were decay corrected. The specific activities were measured at the end of synthesis (EOS).

receptor specificity of this imaging agent. These results are significant as they are the first example showing that the ^{18}F-radiolabelled NHC-BF_3 conjugates can image the targeted tumour *in vivo*. Clearly, the specific activity is high enough for tumour imaging application. However, we do like to point out that the specific activity may need to be improved further for neuroimaging applications where the receptor number is limited.

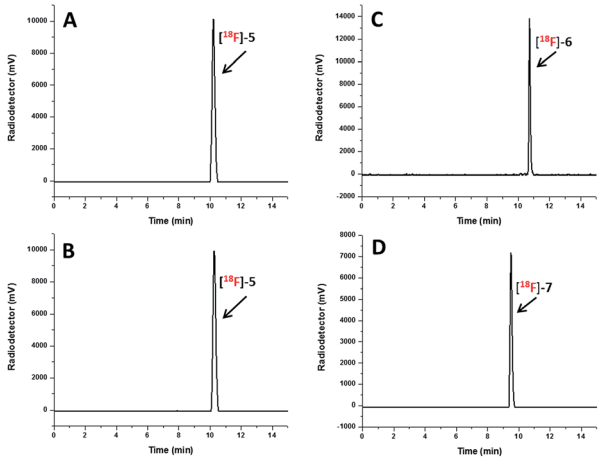

Fig. 3 Radio-HPLC profiles of [^{18}F]**5** after incubation in phosphate buffer solution (PBS) pH = 7.5 for 1 hour (A) and 2 hours (B) and radio-HPLC profiles of [^{18}F]**6** and [^{18}F]**7** after incubation in PBS pH = 7.5 for 2 hours (C and D).

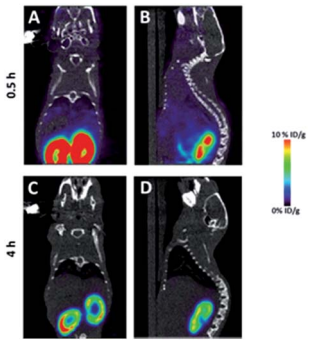

Fig. 4 Decay corrected microPET/CT images of nude mice from a static scan at 0.5 h ((A) coronal image, (B) sagittal image) and 4 h ((C) coronal image, (D) sagittal image) after the injection of [^{18}F]**5**.

The quantification of the activity accumulation in the major organs (Fig. 6A and B) was calculated by measuring the regions of interest (ROIs) encompassing the entire organ. Although the degrees of tumour uptake of [^{18}F]**6** and [^{18}F]**7** are different (1.50 ± 0.013% ID per g for [^{18}F]**6** and 0.54 ± 0.031% ID per g for [^{18}F]**7**), the tumour-to-muscle ratios of both conjugates are

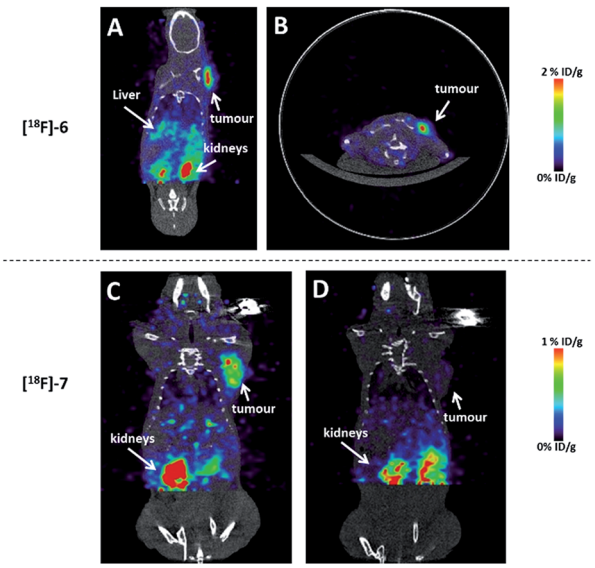

Fig. 5 Above: Decay corrected microPET/CT images of nude mice bearing U87MG tumour from a static scan at 0.5 h after the injection of [^{18}F]**6** ((A) coronal image, (B) transverse image). Below: Decay corrected microPET/CT coronal images of nude mice bearing PANC1 tumour from a static scan at 1 h after the injection of [^{18}F]**7** (C) and [^{18}F]**7** co-injected with 200 μg of NT peptide (D) (blocking experiment).

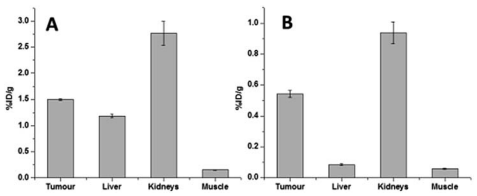

Fig. 6 (A) Bar chart showing microPET quantification of [^{18}F]**6** in nude mice bearing U87MG tumour at 0.5 h post injection. (B) Bar chart showing microPET quantification of [^{18}F]**7** in nude mice bearing PANC1 tumour at 1 h post injection.

comparable (9.85 ± 0.45 for [^{18}F]**6** and 9.33 ± 0.42 for [^{18}F]7) yielding tumour images with good contrast (Fig. 5A and B for [^{18}F]**6**, Fig. 5C for [^{18}F]7). The low liver uptake (0.086 ± 0.0064% ID per g) and the comparatively high kidney uptake (0.94 ± 0.10) of [^{18}F]7 at 1 h post injection indicate that [^{18}F]7 rapidly cleared from liver which is similar to our previous reports on the PET imaging of ^{18}F-vinyl sulfone conjugated NT-peptide.[10]

In summary, we have successfully synthesized [^{18}F]-NHC-BF_3 conjugated bioactive molecules *via* $SnCl_4$ promoted ^{18}F–^{19}F isotopic exchange reaction. This approach allows the fluorine-18 to be introduced at late stage of the synthesis. These agents showed excellent *in vitro* and *in vivo* stability due to the zwitterionic nature of the NHC-BF_3 moiety. As shown in PET imaging, both RGD and NT conjugates ([^{18}F]**6** and [^{18}F]7) demonstrated prominent tumour uptake with good tumour-to-background contrast. This approach provides broad applications for the radiolabelling of thiol-containing bioactive molecules.

Acknowledgements

This work was supported by the National Cancer Institute (P30-CA016086-35-37), and the Biomedical Research Imaging Center, University of North Carolina at Chapel Hill. All animal-related experiments were performed in compliance with the guidelines of Public Health Service (PHS) policy on Human Care and Use of Laboratory Animals approved by the University of North Carolina at Chapel Hill Institutional Animal Care and Use Committee (IACUC).

Notes and references

1 (*a*) K. Chansaenpak, B. Vabre and F. P. Gabbai, *Chem. Soc. Rev.*, 2016, **45**, 954–971; (*b*) D. M. Perrin, *Acc. Chem. Res.*, 2016, **49**, 1333–1343; (*c*) P. W. Miller, N. J. Long, R. Vilar and A. D. Gee, *Angew. Chem., Int. Ed.*, 2008, **47**, 8998–9033; (*d*) A. F. Brooks, J. J. Topczewski, N. Ichiishi, M. S. Sanford and P. J. H. Scott, *Chem. Sci.*, 2014, **5**, 4545–4553; (*e*) V. Bernard-Gauthier, J. J. Bailey, Z. Liu, B. Wängler, C. Wängler, K. Jurkschat, D. M. Perrin and R. Schirrmacher, *Bioconjugate Chem.*, 2016, **27**, 267–279.

2 (*a*) Z. Liu, M. Pourghiasian, F. Bénard, J. Pan, K.-S. Lin and D. M. Perrin, *J. Nucl. Med.*, 2014, **55**, 1499–1505; (*b*) Z. B. Liu, M. A. Radtke, M. Q. Wong, K. S. Lin, D. T. Yapp and D. M. Perrin, *Bioconjugate Chem.*, 2014, **25**, 1951–1962; (*c*) Z. Liu, G. Amouroux, Z. Zhang, J. Pan, N. Hundal-Jabal, N. Colpo, J. Lau, D. M. Perrin, F. Bénard and K.-S. Lin, *Mol. Pharm.*, 2015, **12**, 974–982; (*d*) Z. Liu, M. Pourghiasian, M. A. Radtke, J. Lau, J. Pan, G. M. Dias, D. Yapp, K.-S. Lin, F. Bénard and D. M. Perrin, *Angew. Chem., Int. Ed.*, 2014, **53**, 11876–11880; (*e*) M. Pourghiasian, Z. Liu, J. Pan, Z. Zhang, N. Colpo, K.-S. Lin, D. M. Perrin and F. Bénard, *Bioorg. Med. Chem.*, 2015, **23**, 1500–1506; (*f*) Z. Zhang, S. Jenni, C. Zhang, H. Merkens, J. Lau, Z. Liu, D. M. Perrin, F. Bénard and K.-S. Lin, *Bioorg. Med. Chem. Lett.*, 2016, **26**, 1675–1679; (*g*) Z. Liu, H. Chen, K. Chen, Y. Shao, D. O. Kiesewetter, G. Niu and X. Chen, *Sci. Adv.*, 2015, **1**(8), e1500694; (*h*) Z. Liu, K.-S. Lin, F. Benard, M. Pourghiasian, D. O. Kiesewetter, D. M. Perrin and X. Chen, *Nat. Protoc.*, 2015, **10**, 1423–1432.

3 (*a*) S. Liu, D. Li, Z. Zhang, G. K. Surya Prakash, P. S. Conti and Z. Li, *Chem. Commun.*, 2014, **50**, 7371–7373; (*b*) E. J. Keliher, J. A. Klubnick, T. Reiner, R. Mazitschek and R. Weissleder, *ChemMedChem*, 2014, **9**, 1368–1373.

4 K. Chansaenpak, M. Wang, S. Liu, Z. Wu, H. Yuan, P. S. Conti, Z. Li and F. P. Gabbai, *RSC Adv.*, 2016, **6**, 23126–23133.

5 Z. Li, K. Chansaenpak, S. Liu, C. R. Wade, H. Zhao, P. S. Conti and F. P. Gabbaï, *MedChemComm*, 2012, **3**, 1305–1308.

6 (*a*) S. Liu, T.-P. Lin, D. Li, L. Leamer, H. Shan, Z. Li, F. P. Gabbaï and P. S. Conti, *Theranostics*, 2013, **3**, 181–189; (*b*) K. Chansaenpak, H. Wang, M. Wang, B. Giglio, X. Ma, H. Yuan, S. Hu, Z. Wu and Z. Li, *Chem.–Eur. J.*, 2016, **22**, 12122–12129.

7 K. Chansaenpak, M. Wang, Z. Wu, R. Zaman, Z. Li and F. P. Gabbai, *Chem. Commun.*, 2015, **51**, 12439–12442.

8 (*a*) S. M. Hillier, K. P. Maresca, F. J. Femia, J. C. Marquis, C. A. Foss, N. Nguyen, C. N. Zimmerman, J. A. Barrett, W. C. Eckelman, M. G. Pomper, J. L. Joyal and J. W. Babich, *Cancer Res.*, 2009, **69**, 6932–6940; (*b*) S. M. Hillier, K. P. Maresca, G. Lu, R. D. Merkin, J. C. Marquis, C. N. Zimmerman, W. C. Eckelman, J. L. Joyal and J. W. Babich, *J. Nucl. Med.*, 2013, **54**, 1369–1376; (*c*) Y. Chen, C. A. Foss, Y. Byun, S. Nimmagadda, M. Pullambhatla, J. J. Fox, M. Castanares, S. E. Lupold, J. W. Babich, R. C. Mease and M. G. Pomper, *J. Med. Chem.*, 2008, **51**, 7933–7943.

9 (*a*) D. A. Silver, I. Pellicer, W. R. Fair, W. D. Heston and C. Cordon-Cardo, *Clin. Cancer Res.*, 1997, **3**, 81–85; (*b*) B. S. Slusher, G. Tsai, G. Yoo and J. T. Coyle, *J. Comp. Neurol.*, 1992, **315**, 217–229.

10 Z. Wu, L. Li, S. Liu, F. Yakushijin, K. Yakushijin, D. Horne, P. S. Conti, Z. Li, F. Kandeel and J. E. Shively, *J. Nucl. Med.*, 2014, **55**(7), 1178–1184.